Kufa Journal of Engineering
Vol. 15, No. 4, October 2024, P.P. 186-198
Article history: Received 23 June 2024, last revised 8 July 2024, accepted 10 August 2024

ISOLATING PURE SILICA FROM SYRIAN CLAY FOR BIOGLASS MANUFACTURING

Ahmad Sulaiman[1] and Abdulrazzaq Hammal[*2]

[1] Department of chemistry, College of Science, University of Tartous, Tartous, Syria.

[2*] Department of Basic Sciences, College of Electrical and Electronic Engineering, University of Aleppo, Aleppo, Syria.

[*] Corresponding Author: Abdulrazzaq Hammal

https://doi.org/10.30572/2018/KJE/150412

ABSTRACT

One material that can be used in bone and soft tissue engineering is bioglass. By adhering to bone tissues and forming an apatite layer that further starts the biomineralization process, it can also encourage skin regeneration and wound healing in addition to playing a significant part in the healing processes of bone fractures.In this research, Syrian clay was used as a cheap silica source for preparation bioglass by melting method. Pure silica was isolated by mixing clay with sodium hydroxide in the following amounts (1:1), (2:1), (3:1), treated at different temperatures (700, 800, 900)˚C, treated with HCl solution, filtrated, dried, the yield reached to 96% with purity of 99% when clay was mixed with NaOH by (2:1) and treated at 800˚C. Bioglass was prepared using isolated silica according to thermal program, the formation of bioglass was confirmed by XRD, IR and biodegradability test, which confirmed formation of hydroxyapatite, on the surface which confirmed the biological effectiveness of the prepared bioglass.

KEYWORDS

Biodegradation, Bioglass, Clay, Silica.

1. INTRODUCTION

Biocompatible materials are made specially to work with the human body, helping to evaluate, support, and replace particular organs or tissues. The performance of these materials is assessed according to their compatibility and functionality in the biological environment after implantation, and they are designed for implantation and smooth integration into the body. The ability of these materials to perform a certain physical or mechanical function is known as their biological function, whereas their ability to continue performing this function without endangering or rejecting the surrounding tissues is known as their biological compatibility (Silver, Deas and Erecińska, 2001; Negut, and Ristoscu, 2023; Miguez, Hench and Boccaccini, 2015).

Because of their superior biological compatibility, low porosity, corrosion resistance, and low electrical and thermal conductivity, bioactive materials are highly prized as biologically active materials. By creating a physiologically active hydroxy apatite (HA) layer that closely resembles the chemical and structural makeup of natural bone minerals, bioactive materials create a link with bone tissue and promote interfacial bonding. (Mubina et al., 2021; Shan et al., 2020; Crovace et al., 2021; Dimitriadis et al., 2021; Wetzel et al., 2020)

Composed of 45% SiO_2, 24.5% CaO, 24.5% Na_2O, and 6% P_2O_5, the 45S5 bioactive glass system is the most bone bonding constituents. When exposed to human plasma or comparable fluids, the highly reactive surface of this bioactive glass interacts actively, forming a silica gel sheet and causing a calcium phosphate sheet to precipitate (Lefebvre et al., 2007; Satyendra et al., 2024; Abbasi and Hashemi, 2014).

For bioactive glass, there are two primary preparation techniques that are frequently discussed: melt-quench and sol-gel. The desired qualities and their intended uses determine the post-treatment that is applied to the samples. Notably, both the creation of contaminant-free products and the purity of the raw materials are essential. While bioactive glass made using the sol-gel approach is more porous and has a greater specific surface area, melting-quenching reduces the specific surface area and creates bioactive glass with a soft and low porosity on their surface (Srinath et al., 2020; Et al., S. 2019).

Large-scale production of bioactive glasses is significantly hampered by the costly and hazardous nature of the commonly used alkoxysilane precursors, such as tetraethyl orthosilicate (TEOS) and tetramethyl orthosilicate (TMOS), despite the fact that the sol-gel method has several advantages over the melt and solidification method, including greater homogeneity and purity as well as a greater variety of compositions (Kaou et al., 2023; Pajares and Chatzistavrou, 2020; Shearer, Montazerian and Mauro, 2022; Abd Dleam, and Kareem, 2021).

As a result, in their quest for large-scale bioactive glasses, some research has looked into alternate sources of silica. In order to create bioactive materials, silica has been extracted from a variety of industrial and agricultural wastes, particularly egg shells, rice straw, and soda-lime-silica waste glass (Essien et al., 2013).

Clay minerals are fine-grained hydrous silicates with an octahedral or tetrahedral layered configuration, and recent research has included using them as precursor materials for the creation of bioactive glass (Essien et al., 2013)**,** their chemical composition implies that they may yet serve as an economically viable non-toxic silica source for large scale synthesis of bioactive glasses.

Sedimentary clay with a three-layered structure is a naturally occurring clay mineral that is created when volcanic ash weathers. It shows two silicon oxide sheets encasing one aluminum oxide layer. Fig 1. In terms of structure, the external silicon oxide sheet and the inside aluminum share oxygen atoms, and Mg^{2+} ions frequently replace Al^{3+} ions, producing a net negative charge. Counter ions, often Na^{+} and Ca^{2+}, that are found between platelets balance the charge in the platelets. The silicon oxide in clay minerals can be removed using alkali at a high temperature to get the equivalent alkali silicate, which might be used as a precursor for the manufacture of glass (Battaglia, Cuevas, and De Wolf, 2016; Tawfiq and Asaad, 2021; Bakhshi, Mozdianfard, and Hayati, 2020).

This study aims to use Syrian clay as a cheap silica source for preparation a type of bioglass by melting method, as no previous study has used this raw material to produce bioactive glass.

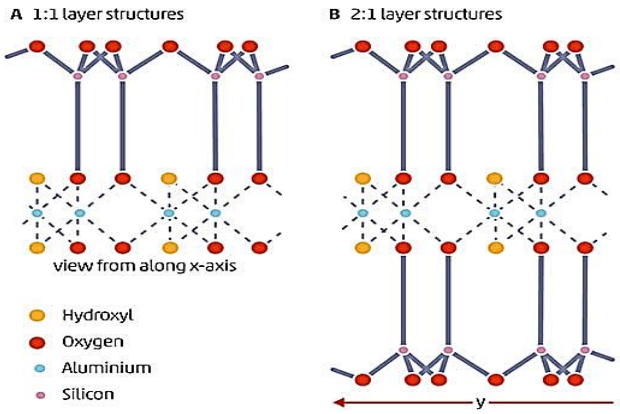

Fig. 1. Crystal structure of clay mineral 1:1 layer and 2:1 layer (Battaglia, Cuevas, and De Wolf, 2016)

2. MATERIALS AND METHODS

Raw clay samples

Raw clay was gathered in Syria's Wadi Al-Zakara region. A porcelain mill was used to grind the raw clay, and particles smaller than 100µm were separated using a standard sieve and an electric vibrator manufactured by Retch Model (AS.200). X-ray fluorescence (XRF) analysis

was used to determine the raw clay's chemical composition, and X-ray diffraction (XRD) with a nickel filter and Cu Kα1 radiation (λ=1.5405°A) from a (BRUKER AXS Diffractometer D8) was used to identify the crystal phases.

Isolating pure silica from clay

An electric oven with multiple heating systems, manufactured by Carbolite, was used to thermally treat the mixtures of clay: NaOH (1:1) (2:1) (3:1) at various temperatures (700, 800, and 900)˚C. The mixtures were placed in a carbon crucible, temperature was gradually increased at a rate of 10 degree per minutes until it reached (700, 800, or 900)˚C. The temperature was fixed for 60 minutes, mixtures were cool gradually. Subsequently, each combination was heated to 80˚C and treated with a 2:1 diluted hydrochloric acid to separate silica (as H_2SiO_3) from the remaining compounds. Filtered and washed with distilled water, dried at 105˚C, to yield silica (1):

$$H_2SiO_3 \rightarrow H_2O\uparrow + SiO_2 \quad (1)$$

silica yield was calculated as (2):

$$S_p\% = (W_s / W_c)x\ 100 \quad (2)$$

Where: S_p%: silica yield, %.W_s: silica weight, W_c: t of clay's silica weigh.

Isolated silica was examined with XRF, the distance between the crystal planes determined by Miller's clues (hkl) was calculated based on Bragg's law (3):

$$n\lambda=2d\sin\theta \quad (3)$$

Where:

The distance between parallel planes was computed using the crystal lattice constants of the tetragonal structure and the lattice constants in accordance with (4). The variables were d: distance between parallel crystal planes, θ: diffraction angle, n: diffraction order, and λ wavelength of X-ray (λ=1.540A˚).

$$1/d^2 = (h^2+k^2/a^2) +(l^2/c^2) \quad (4)$$

Based on the Debye-Scherer connection, calculate the stress or tension coefficient (crystal lattice strain ε) and the density of dislocations using (5):

$$D = K\lambda/\beta\cos\theta \quad (5)$$

where: D is the size of the crystalline grains; K is a constant equal to 0.94 in the case of spherical particles; and βhkl is the mid-intensity breadth of the diffraction peak corresponding to the plane hkl. Using (6), the δ density of dislocations was computed (Abd Dleam, and Kareem, 2021; Battaglia, Cuevas, and De Wolf, 2016):

$$\delta = n/D^2 \quad (6)$$

To get the lowest value for the density of dislocations, where n is a constant equal to one. Additionally, using (7), the stress or tension coefficient (crystal lattice strain ε) was determined (Abd Dleam, and Kareem, 2021; Battaglia, Cuevas, and De Wolf, 2016).

$$\varepsilon = \beta \cos\theta/4 \quad (7)$$

Preparation of bioglass

45S5 glass, which is regarded as one of the glass systems with biological qualities and is a member of the glass system ($CaO.P_2O_5.SiO_2$), was made using the silica that was isolated for this study as shown in Table 1 (Satyendra et al., 2024). For preparation 45S5, the same glass combination was made using pure ingredients from Sigma-Aldrich: calcium phosphate $Ca_3(PO_4)_2$ (99%), sodium carbonate Na_2CO_3 (98%), and calcium carbonate $CaCO_3$ (99%), as indicated in Table 2.

Table 1. Composition of 45S5 (Satyendra et al., 2024)

W%			Σ(%)	
SiO_2	CaO	P_2O_5	Na_2O	100
45.0	24.5	6.0	24.5	

Table 2. Chemical precursors for syntheses 45S5

W(gr)				Σ(gr)
SiO_2	$CaCO_3$	$Ca_3(PO_4)_2$	Na_2CO_3	132.42
44.13	31.29	13.26	42.19	

The mixture's moisture content was eliminated through thermal processing. At a pace of 10 degrees per minute, the temperature was raised progressively to 200°C and maintained there for 30 minutes. The temperature was gradually raised to 1100°C at a pace of 15 degrees per minute in order to stop the mixture's constituent parts from dispersing as a result of the carbon dioxide being released. This temperature was held for 60 minutes while monitoring the melting of the sample. After that, it was raised by 20 degrees per minute and held for 35 minutes at 100°C intervals. The sample completely melted ten minutes after the temperature hit 1300°C. The thermal program utilized to create bioglass is depicted in Fig 2. (An experimental program that was concluded after several experiments).

The Bruker Vector 22 FTIR spectrometer was used to measure the IR spectra of the prepared samples in the 4000–400 cm^{-1} range after the prepared bioglass was characterized by XRD.

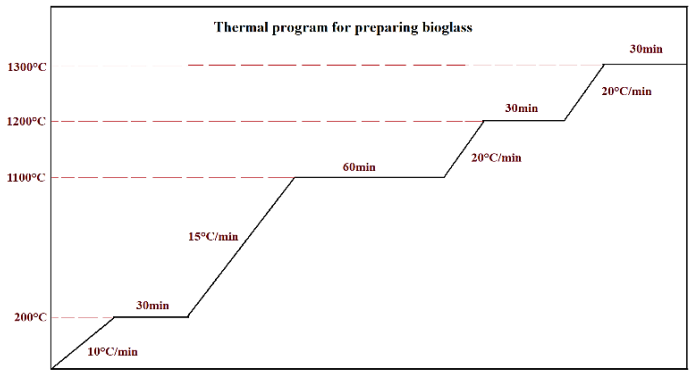

Fig. 2. Thermal program to synthase sample

Biodegradability of prepared bioglass

For synthetic biomaterials, biodegradation is essential because it should coincide with tissue regrowth. Si^{4+}, P^{5+}, and Ca^{2+} ions are essential for tissue function. In order to investigate biodegradability in the lab, prepared bioglass was crushed into a powder, soaked in the "simulated body fluid" solution (SBF) for 7, 14, 21, 28, and 35 days, placed in an incubator set at 37°C. Bioglass mostly degrades by dissolving in surrounding medium. The investigations included in Table 3 served as the foundation for the creation of the SBF solution Table 3 (Yadav, Singh, and Pyare, 2020).

The ratio of SBF solution to powder was measured at 50:1. On several days, the pH was monitored, and the biodegradability equation was computed using the following formula:

$\%W_L = W_0 – W_1/W_0$, where W_0 the sample's weight prior to sinking in SBF, W_1 the sample's dry weight following SBF dipping, and $\%W_L$ is the percentage of weight loss. (Yadav, Singh, and Pyare, 2020)

Table 3. components of SBF

Substances	Weight
NaCl	7.91 gr
$NaHCO_3$	0.33 gr
$K_2HPO_4.3H_2O$	0.24 gr
KCl	0.25 gr
$MgCl_2.6H_2O$	0.30 gr
$CaCl_2$	0.27 gr
Na_2SO_4	0.08 gr
HCl 1M	43 ml
$NH_2C(CH_2OH)_3$	7.94 gr

3. RESULTS AND DISCUSSION

In accordance with the siliceous structure of clays, silicon dioxide (SiO_2) made up 49.34% of the clay sample, according to chemical analysis. Aluminum oxide (Al_2O_3) made up 17.15% of the components of the clay under study Table 3. Clay's XRD patterns in Fig 3 revealed that the main minerals it contains were quartz, illite, and kaolinite.

Table 4. Chemical composition of clay

Compound	Clay%
SiO_2	49.34
Al_2O_3	17.15
Fe_2O_3	7.85
MgO	2.12
CaO	7.48
Na_2O	0.19
K_2O	1.35
L.O.I	12.85

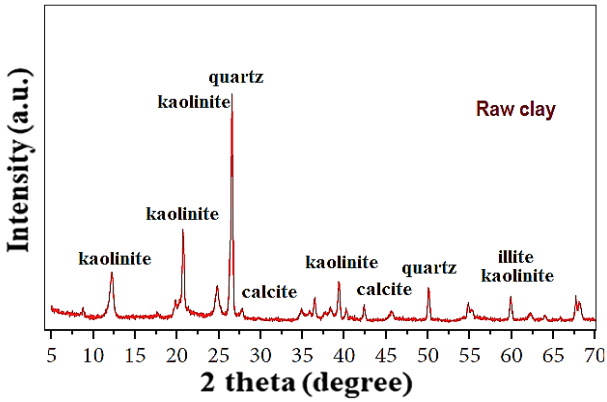

Fig. 3. XRD of Clay sample

When utilizing a clay:sodium hydroxide mixtures of (2:1) and (3:1) and proses at (800 or 900)˚C, the yield of silica was 96%, with a purity of up to 99%. This suggests that the process used to create silica in this study was successful. Because it produced heterogeneous agglomerates and had a poor silica yield (no more than 39%), the mixing ratio (1:1) was disregarded, indicating that the clay did not completely disintegrate. Varied agglomerates were also produced by thermally treating the clay and sodium hydroxide mixtures at 700°C.

When comparing the prepared silica's XRD spectrum with the reference XRD spectrum in Fig4, it was observed that there was perfect agreement between the prepared silica's peaks and the reference code No. 00-046-1045. This indicates the prepared silica's purity Table 5, Table 6.

Table 5. Chemical analysis of extracted silica

Component	W%
SiO_2	99.02
Al_2O_3	0.08
Fe_2O_3	0.07
CaO	0.06
MgO	0.08
SO_3	0.01
K_2O	0.05
Na_2O	0.05
L.I.O	0.03

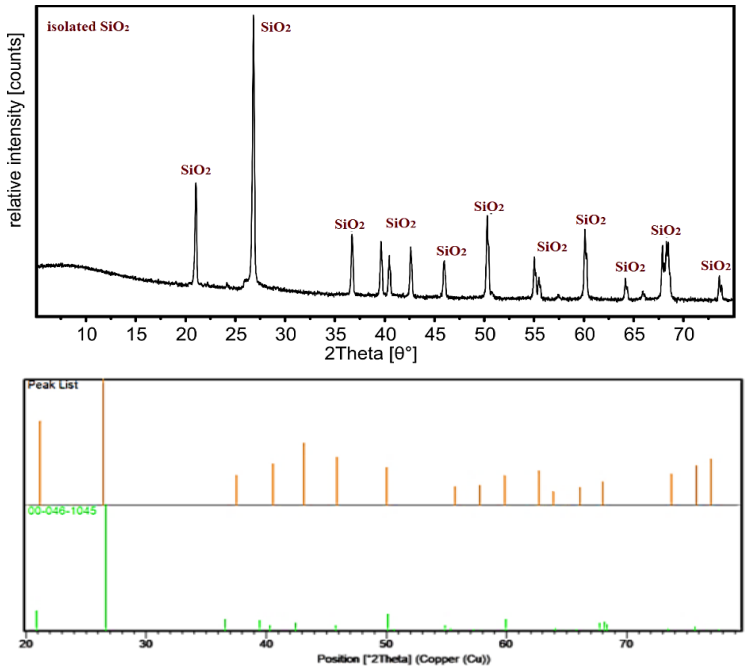

Fig. 4. XRD spectrum of isolated SiO_2

Table 6. properties of extracted silica

Sample	2θ	hkl	d (A°)	D(nm)	δ 10^{15} (lines$.m^{-2}$)	ε (10^{-4} line $s^{-2}.m^{-4}$)	β^{o}_{hkl}
Isolated SiO_2	26.452	101	3.369	9.8	10.4	35.78	0.8423

XRD spectrum of bioglass that has been prepared The absence of peaks in Fig 5 that would have suggested the existence of a crystalline constituent validates the development of a glass phase, results of the generated bioglass's IR spectra in Fig 6 were in agreement with earlier research (Xanthippi et al., 2004.).

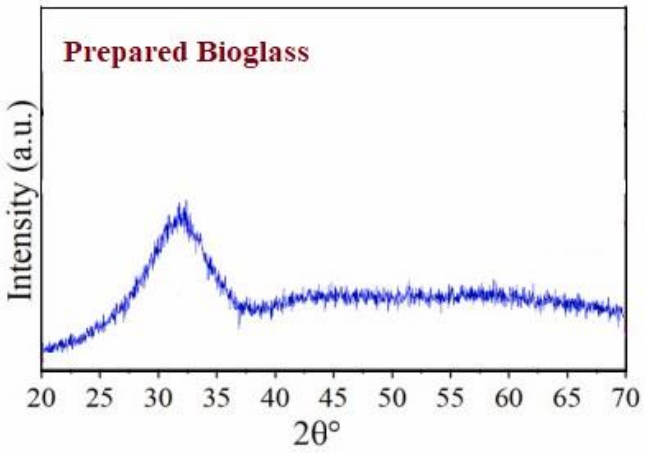

Fig. 5. XRD spectrum of syntheses bioglass

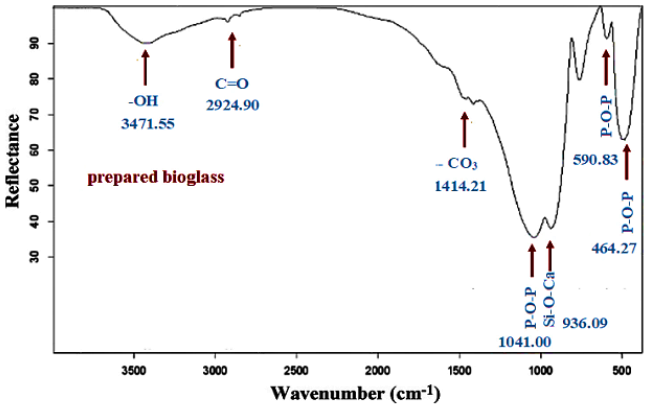

Fig. 6. FTIR spectrum of syntheses bioglass

Because of the ionic interaction between the prepared bioglass and the constituents of the SBF, the weight loss increased over the course of the 28-day SBF immersion period, reaching 9.8% before nearly stabilizing at 9.9%. As a result, the pH of the SBF solution increased to 8.4 during the first 14 days and then stabilized with longer soaking times Fig7 (Xanthippi et al., 2004.). The alkaline pH increased osteoblast cell proliferation, according to the previous report. When phosphate and calcium are present in these precise molar ratios during the bioglass preparation process, a layer of hydroxyapatite forms. Once HA forms, the pH stays comparatively constant as the immersion time rises, as shown in Fig 8.

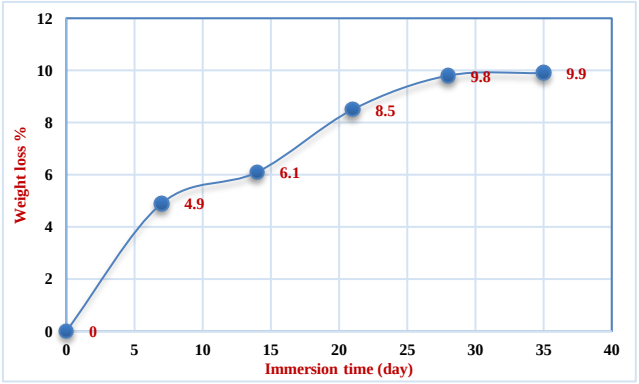

Fig. 7. Weight loss in SBF

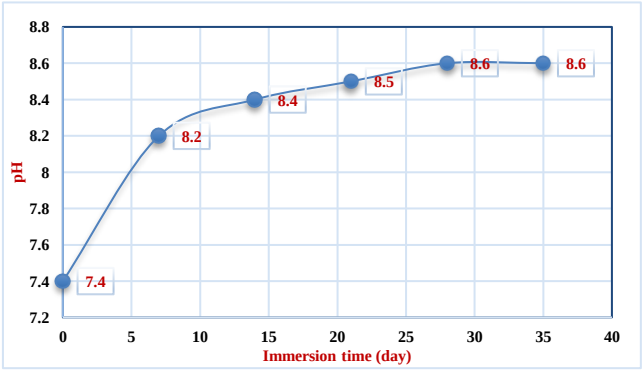

Fig. 8. pH during soaking

The white layer that developed on the surface of bioglass submerged in SBF solution was separated, dried, and its composition was ascertained using XRD. The peaks in the XRD were used to demonstrate the production of hydroxyapatite. After the prepared bioglass was submerged in SBF solution, Fig 9 showed that the hexagonal hydroxyapatite Ca5(PO4)3OH phase with card number 00-001-1008 was present. The main (hkl) indices for the formed layer hydroxyapatite were (002), (211), (112), (300), (202), (222), (004), and (223), which validated the prepared glass's biological efficacy. Research steps are shown in Fig 10.

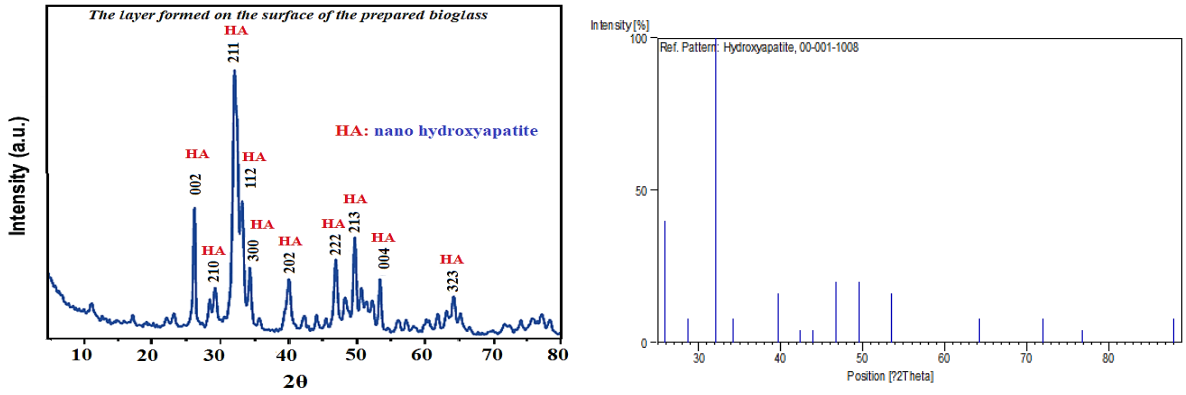

Fig. 9. XRD of the formed layer on surface of the prepared bioglass and reference cod

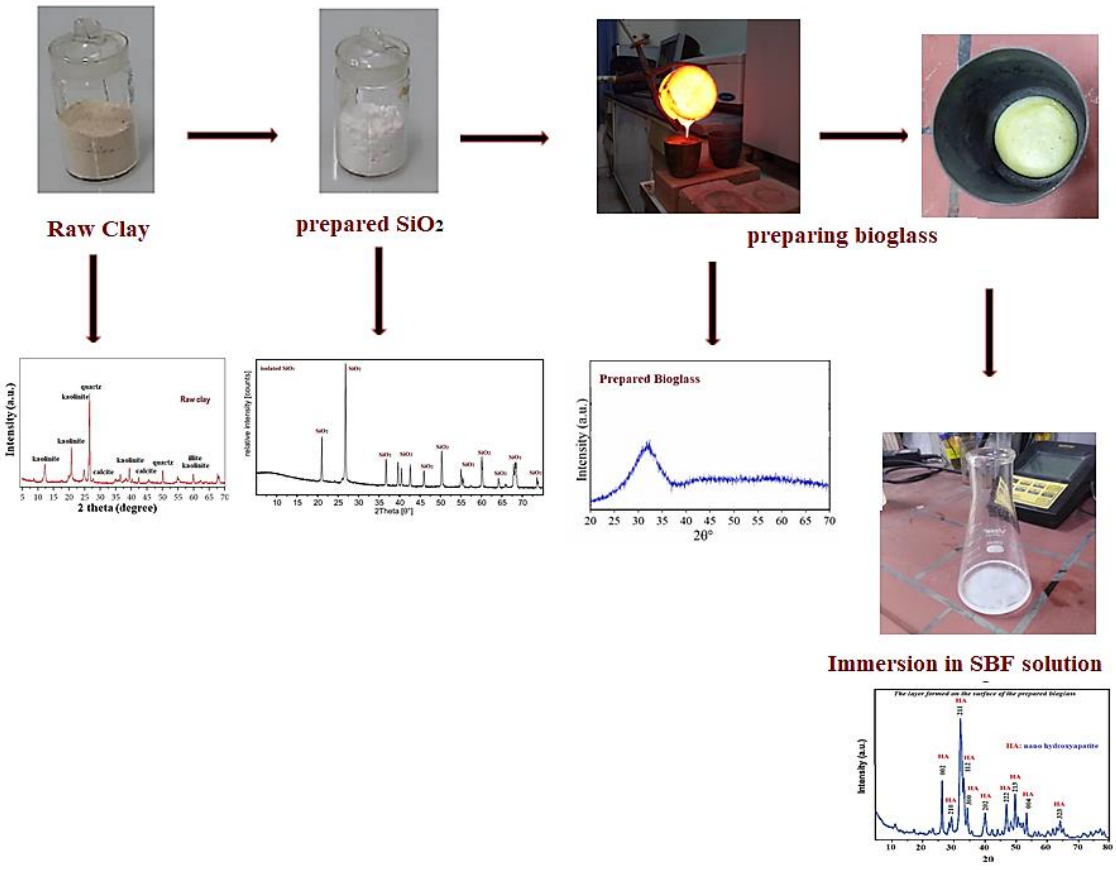

Fig. 10. Research steps

4. CONCLUSION

Pure silica was isolated from Syrian clay as a cheap silica source for preparation of bioglass by melting method, isolated was prepared by mixing clay with sodium hydroxide in the following percent (1:1), (2:1), and (3:1), then treated at different temperatures (700, 800, 900)˚C, treated with HCl solution, filtrated, dried, the yield reached to 96% with purity of 99% when clay was mixed with NaOH by (2:1) and treated at 800˚C.

Bioglass was prepared using isolated silica according to thermal program, the formation of bioglass was confirmed by XRD, IR and biodegradability test, which confirmed formation a layer of hydroxyapatite on the surface of the bioglass immersed in SBF solution.

The specifications of the prepared bioglass make it usable in some related medical applications such as bone tissue restoration, dental fillings, etc.

Authors' Declaration

- Conflicts of Interest: None.
- We hereby confirm that all the Figures and Tables in the manuscript are ours. Furthermore, any Figures and images, that are not ours, have been included with the necessary permission for re-publication, which is attached to the manuscript.

5. REFERENCES

Abbasi, M. and Hashemi, B. (2014). Fabrication and characterization of bioactive glass-ceramic using soda–lime–silica waste glass. Materials Science and Engineering: C, 37, pp.399–404. doi: https://doi.org/10.1016/j.msec.2014.01.031.

Abd Dleam, E., & Kareem, S. H. (2021). Mesoporous Silica Nanoparticles as a System for Ciprofloxacin Drug Delivery; Kinetic of Adsorption and Releasing. (2021). Baghdad Science Journal, 18(2). doi: https://doi.org/10.21123/bsj.2021.18.2.0357.

Bakhshi, M., Mozdianfard, M.-R. and Hayati-Ashtiani, M. (2020). INVESTIGATING MINERALOGICAL AND PHYSIO-CHEMICAL PROPERTIES OF BENTONITE FOR WATER-BASED FLUIDS. Kufa Journal of Engineering, 11(1), pp.79–89. doi: https://doi.org/10.30572/2018/kje/110106.

Battaglia, C., Cuevas, A. and De Wolf, S. (2016). High-efficiency crystalline silicon solar cells: status and perspectives. Energy & Environmental Science, 9(5), pp.1552–1576. doi: https://doi.org/10.1039/c5ee03380b.

Crovace, M.C., Soares, V.O., Rodrigues, A.C.M., Peitl, O., Raucci, L.M.S.C., de Oliveira, P.T. and Zanotto, E.D. (2021). Understanding the mixed alkali effect on the sinterability and in vitro

performance of bioactive glasses. Journal of the European Ceramic Society, 41(7), pp.4391–4405. doi: https://doi.org/10.1016/j.jeurceramsoc.2020.11.020.

Dimitriadis, K., Tulyaganov, D.U., Vasilopoulos, K.C., Karakassides, M.A. and Agathopoulos, S. (2021). Influence of K and Mg substitutions on the synthesis and the properties of CaO-MgO-SiO2/Na2O, P2O5, CaF2 bioactive glasses. Journal of Non-Crystalline Solids, 573, p.121140. doi: https://doi.org/10.1016/j.jnoncrysol.2021.121140.

Essien, E.R., Adams, L.A., Shaibu, R.O. and Oki, A. (2013). Sol-gel bioceramic material from bentonite clay. Journal of Biomedical Science and Engineering, 06(03), pp.258–264. doi: https://doi.org/10.4236/jbise.2013.63032.

Et al., S. (2019). Synthesis of Functionalized Silica from Rice Husks Containing C-I End Group. Baghdad Science Journal, 16(4), p.0886. doi: https://doi.org/10.21123/bsj.2019.16.4.0886.

Kaou, M.H., Mónika Furkó, Katalin Balázsi and Csaba Balázsi (2023). Advanced Bioactive Glasses: The Newest Achievements and Breakthroughs in the Area. Nanomaterials, 13(16), pp.2287–2287. doi: https://doi.org/10.3390/nano13162287 .

Lefebvre, L., Chevalier, J., Gremillard, L., Zenati, R., Thollet, G., Bernache-Assolant, D. and Govin, A. (2007). Structural transformations of bioactive glass 45S5 with thermal treatments. Acta Materialia, 55(10), pp.3305–3313. doi: https://doi.org/10.1016/j.actamat.2007.01.029.

Miguez-Pacheco, V., Hench, L.L. and Boccaccini, A.R. (2015). Bioactive glasses beyond bone and teeth: Emerging applications in contact with soft tissues. Acta Biomaterialia, 13, pp.1–15. doi: https://doi.org/10.1016/j.actbio.2014.11.004.

Mubina, M.S.K., Shailajha, S., Sankaranarayanan, R. and Smily, S.T. (2021). Enriched biological and mechanical properties of boron doped SiO2-CaO-Na2O-P2O5 bioactive glass ceramics (BGC). Journal of Non-Crystalline Solids, 570, p.121007. doi: https://doi.org/10.1016/j.jnoncrysol.2021.121007.

Negut, I. and Ristoscu, C. (2023). Bioactive Glasses for Soft and Hard Tissue Healing Applications—A Short Review. Applied sciences, 13(10), pp.6151–6151. doi: https://doi.org/10.3390/app13106151.

Pajares-Chamorro, N. and Chatzistavrou, X. (2020). Bioactive Glass Nanoparticles for Tissue Regeneration. ACS Omega, 5(22), pp.12716–12726. doi: https://doi.org/10.1021/acsomega.0c00180.

Satyendra Kumar Singh, Kumar, J., Singh, P., Rajput, S.K., Ashutosh Kumar Dubey, Ram Pyare and Roy, P.K. (2024). Impact of 13-93 bio-glass inclusion on the machinability, in-vitro degradation, and biological behavior of Y-TZP-based bioceramic composite. Ceramics International, 50(1), pp.1087–1106. doi: https://doi.org/10.1016/j.ceramint.2023.10.203.

Shan, Z., Zhang, Y., Liu, S., Tao, H. and Yue, Y. (2020). Mixed-alkali effect on hardness and indentation-loading behavior of a borate glass system. Journal of Non-Crystalline Solids, 548, pp.120314–120314. doi: https://doi.org/10.1016/j.jnoncrysol.2020.120314.

Shearer, A., Montazerian, M. and Mauro, J.C. (2022). Modern Definition of Bioactive Glasses and Glass-Ceramics. arXiv:2212.00213 [cond-mat, physics:physics]. [online] doi: https://doi.org/10.1016/j.jnoncrysol.2023.122228.

Silver, I.A., Deas, J. and Erecińska, M. (2001). Interactions of bioactive glasses with osteoblasts in vitro: effects of 45S5 Bioglass®, and 58S and 77S bioactive glasses on metabolism, intracellular ion concentrations and cell viability. Biomaterials, 22(2), pp.175–185. Doi: https://doi.org/10.1016/s0142-9612(00)00173-3.

Srinath, P., K. Venugopal Reddy, Patel, S. and P. Abdul Azeem (2020). A cost effective SiO2–CaO–Na2O bio-glass derived from bio-waste resources for biomedical applications. Progress in Biomaterials, [online] 9(4), pp.239–248. doi: https://doi.org/10.1007/s40204-020-00145-0.

Tawfiq Aamir Jawad and Asaad Mohammed Baqir (2021). Improvement Of Sandy Soil Properties By Using Bentonite., 1(1), pp.29–39. doi: https://doi.org/10.30572/2018/kje/11289.

Wetzel, R., Blochberger, M., Scheffler, F., Hupa, L. and Brauer, D.S. (2020). Mg or Zn for Ca substitution improves the sintering of bioglass 45S5. Scientific Reports, 10(1). doi: https://doi.org/10.1038/s41598-020-72091-7.

Xanthippi Chatzistavrou, T. Zorba, Eleana Kontonasaki, K. Chrissafis, Petros Koidis and Paraskevopoulos, K.M. (2004). Following bioactive glass behavior beyond melting temperature by thermal and optical methods. Physica status solidi, 201(5), pp.944–951. doi: https://doi.org/10.1002/pssa.200306776.

Yadav, S., Singh, P. and Pyare, R. (2020). Synthesis, characterization, mechanical and biological properties of biocomposite based on zirconia containing 1393 bioactive glass with hydroxyapatite. Ceramics International, 46(8), pp.10442–10451. doi: https://doi.org/10.1016/j.ceramint.2020.01.043.